The effects of growth differentiation factor 15 deficiency on the development of the human placenta

by
Shirley Morris

A thesis submitted to the Department of Biological Sciences, University of Manitoba,

in partial fulfilment of the requirements for the course

BIOL 4100 (Honours Thesis)

for the degree of

Bachelor of Science (Honours)

©April, 2026

Abstract

The placenta plays critical endocrine roles in the health of the mother and fetus. Therefore, characterizing the sources of adherent placental development has implications for improving pregnancy outcomes with potential applications in miscarriage treatment and the diagnosis of congenital conditions prenatally. Placentally produced growth differentiation factor 15 (GDF15) is a promising candidate for study, and previous research in the Xing lab has correlated its peak expression with critical neurodevelopmental timepoints. However, studying this factor in human placental development is complicated by the inaccessibility of human samples and the lack of similarities between human and non-human placentas. Luckily, trophoblast organoids serve as excellent model systems for recapitulating development. Beginning with placental stem cells, some of which have been genetically modified to possess GDF15-deficient genotypes, previously published protocols can be followed to generate organoids to compare stem (cytotrophoblast, CT) and differentiated (syncytiotrophoblast, ST) cell populations. Using an EdU cell proliferation assay, my project found that GDF15 deficiency causes a dramatic reduction in CT cell proliferation and that supplementation by recombinant GDF15 may provide a rescue effect for homozygous GDF15 knock-out (KO) cells. Immunofluorescent staining and quantification of KO and wild-type (WT) organoids show that KO organoids contain a higher proportion of ST cells compared to WT organoids. Together, this provides evidence for the role of GDF15 in maintaining proliferative capacities in placental stem cells. In its absence, cells are more likely to differentiate, potentially leading to placental defects as the stem cell population is exhausted early.

Acknowledgements

I would first like to thank my advisor, Dr. Lei Xing, for his guidance and dedication to this project, as well as my committee members, Dr. John Markham and Dr. Margaret Docker, for their contributions to this thesis. Thank you to the members of the Xing lab—Ho In Shin, Sounak Ray, Aya Tuma, Erica Wong, and Kalan Azaransky—for their help and friendship. Lastly, thank you to my family and friends who supported me outside of the lab.

Table of Contents

1. **Introduction** 1

2. **Research objectives** 5

3. **Methods and Materials** 5

3.1 *Trophoblast stem cell culture* 5

3.2 *Trophoblast organoid culture* 9

3.3 *Cell proliferation assay* 11

3.4 *Immunofluorescence* 13

3.5 *Statistical analysis* 14

4. **Results** 14

4.1 *Establishment of CT29 cell 2D culture* 14

4.2 *GDF15 deficiency impairs CT29 cell growth* 17

4.3 *GDF15 deficiency decreases CT29 cell proliferation* 21

4.4 *Establishment of 3D trophoblast organoid culture* 23

4.5 *Area of WT, KO, and GDF15$^{+/-}$ organoids* 26

4.6 *Ratio of CT and ST cells in WT and KO organoids* 28

5. **Discussion** 32

6. **References** 40

List of Tables

Table 1. Multiwell cell culture plate size, the amount of Geltrex^{TM} used, and the amount of media used in each well. 6

Table 2. Reagents used for 2D CT29 cell culture.. 8

Table 3. Reagents used for trophoblast organoid culture.. 10

Table 4. Cell clones used for the cell proliferation assay. 12

Table 5. Average area of WT, KO, and GDF15$^{+/-}$ organoids grown in two batches. 27

List of Figures

Figure 1. Model setup of the 2D CT29 cell culture and 3D trophoblast organoid culture……11

Figure 2. Light microscopic images of typical CT29 cell growth taken at 4X magnification.....16

Figure 3. Image of a WT CT29 cell cluster taken at 10X magnification 17

Figure 4. Growth curves of different CT29 cell clones.....21

Figure 5. GDF15 regulates CT29 cell proliferation.. 22

Figure 6. Brightfield images of trophoblast organoids and droplets in culture.....25

Figure 7. Brightfield images of trophoblast organoids in culture.....26

Figure 8. Representative images of WT (Clone 4) and KO (Clone 7) organoids stained with CDH1 (pink), CGB3 (green), and DAPI (grey) 28

Figure 9. GDF15 deficiency increases the proportion of ST cells in trophoblast organoids 31

1. Introduction

The placenta, a critical bridge between mother and fetus, forms during the first trimester, beginning its development shortly after fertilization and remaining active throughout the pregnancy before being expelled at birth (Herrick & Bordoni, 2023). The blastocyst, whose inner cell mass will later form the embryo proper, initiates placental development when the trophectoderm, its outermost layer, connects to the epithelium of the endometrium and begins producing cytotrophoblast (CT) stem cells (Mischler et al., 2021; Turco & Moffett, 2019). Once the blastocyst has fully invaded the endometrium, now termed the decidua, the CT cells begin differentiating into syncytiotrophoblast (ST) cells, which form a specialized cell mass called the primary syncytium (Li et al., 2023; Turco &Moffett, 2019). The primary syncytium moves through the decidua, eroding maternal capillaries and glands to form fluid-filled cavities called lacunae (Turco &Moffett, 2019). The remaining CT cells below the primary syncytium soon begin pushing through it, forming primary villi, which break up the lacunae into intervillous spaces. The cores of these villi are formed from CT cells, while the outer layer differentiates into more ST cells. The villi begin branching, forming tree-like structures with more surface area to contact the maternal blood. CT cells that have travelled to the end of the primary syncytium merge to encircle the blastocyst and villi, dividing them from the decidua. From there, some CT cells can differentiate into extravillous trophoblast (EVT) cells, which travel further into the decidua. The primary villi become secondary villi as embryonic mesenchymal cells move through the core, and tertiary villi as that core develops blood vessels (Turco &Moffett, 2019).

The fetal villi are surrounded by maternal blood, and the fetal EVTs extend deeply into the maternal decidua, providing numerous interfaces between the fetus and the

mother. (Turco & Moffett, 2019). These connections are critical for gas, nutrient, and waste exchange (Novakovic, 2013). The placenta also produces essential hormones and other cell-extrinsic factors necessary for fetal development (Rosenfeld, 2021). If endocrine issues arise within the placenta, the fetus may be gravely affected, potentially resulting in lifelong health conditions or pregnancy difficulties such as preeclampsia, preterm birth, or even stillbirth (Li et al., 2023). The fetal brain is particularly vulnerable to placental dysfunction, and many neurotransmitters are produced solely in the placenta during the initial development of the fetal brain (Rosenfeld, 2021). This relationship is described as the placenta-brain axis and highlights the critical role of the placenta as a neuroendocrine organ. Notably, the placenta produces serotonin, dopamine, and epinephrine, which greatly affect fetal brain development at the earliest stages (Rosenfeld, 2021). Glucocorticoids, extracellular vesicles containing microproteins and miRNAs, and numerous growth factors also travel from the placenta to the fetal brain, impacting development (Gumusoglu, 2024). Neurological conditions such as autism spectrum disorder, anxiety, and schizophrenia have been connected to placental endocrine factor disruptions and clarifying how placental endocrine function affects the fetal brain could lead to advancements in early detection and treatment of neurological conditions (Gumusoglu, 2024; Sato, 2013).

Studies exploring the roles of specific placental secretions on the developing brain have begun to emerge (Kay et al., 2018; Vacher et al., 2021; Zeng et al., 2023). For example, insufficient levels of the placental steroid allopregnanolone have been shown to negatively affect cerebral white matter development, causing autism-like symptoms in mice (Vacher et al., 2021). Likewise, low levels of proangiogenic placental growth factor (PGF) in mice hinder brain development, leading to poor spatial learning and less

exploratory behaviour (Kay et al., 2018). Low levels of growth differentiation factor 15 (GDF15) have been linked to miscarriage in humans and embryo reabsorption in mice (Zeng et al., 2023). GDF15 seems to contribute to disordered placentation, which frequently results in miscarriage; however, the precise mechanisms by which this occurs are still unclear (Zeng et al., 2023).

GDF15 is a member of the transforming growth factor β (TGF-β) cytokine superfamily and is expressed in many organs, but never so much as in the placenta, making it of particular interest when studying this endocrine organ (Iglesias et al., 2023). GDF15 is produced by ST cells and plays a role in proper trophoblast migration and their invasion into the decidua following embryo implantation (Zeng et al., 2023). It is also known that elevated levels of placental GDF15 cause increased nausea and vomiting in pregnant women, a condition called hyperemesis gravidarum (Fejzo et al., 2023). GDF15 likely has wide-reaching effects on the experience and outcome of pregnancy, and research is ongoing to examine its effects on the fetus, mother, and placenta. Analysis of human and murine placental samples shows a significant increase in GDF15 expression in the placenta during the peak of neural progenitor cell proliferation (post-conceptional weeks 9 to 11), indicating the importance of GDF15 at the earliest stages of brain development (Shin et al., 2026). These findings raise questions concerning how GDF15 deficiency alters the placenta and how those changes may affect the fetus.

Critical to answering these questions are representative models that recapitulate human placental development (Li et al., 2023). Physiological and anatomical differences limit the use of animal models (Carter, 2007; Li et al., 2023). In particular, the molecular mechanisms controlling placentation and the degree to which trophoblast cells invade the decidua differ greatly between species, with notable differences seen even between

humans and other primates (Carter, 2007). Although cells isolated from human placentae following birth have the same physiology and expression profile as *in vivo* cells, the third-trimester CT cells do not proliferate, and cultures of these cells are often contaminated with other cell types, such as fibroblasts (Nursalim et al., 2021). Moreover, the use of human tissue is heavily regulated, and fresh samples are required frequently to maintain CT cell cultures derived from term placentae (Li et al., 2023). Furthermore, 2D cell cultures do not model the 3-dimensional structure of the placenta, notably the villi, limiting their research applications (Li et al., 2023). Organoids grown from human trophoblast stem cells share many similarities with the placenta, with different protocols modelling different trimesters. Trophoblast organoids display the same cell types and tissue architecture as the placenta and can be genetically manipulated and generated indefinitely from stem cell cultures (Li et al., 2023; Sheridan et al., 2020). Organoids offer the closest approximation to *in vivo* tissues, which, while theoretically ideal, are not readily accessible nor feasible tools for all experiments.

Organoid technology is still relatively new, but it is already evident that it overcomes many limitations to the study of organ development and disease, making them exciting model systems (Kim et al., 2020). Protocols for generating organoids vary depending on the organ they model. In general, embryonic or induced pluripotent stem cells are expanded in a 2D culture before being aggregated in a solution rich with extracellular matrix components, which provide basement-membrane signals and the necessary 3-dimensional support for the stem cells to self-organize into organoids (Corsini & Knoblich, 2022; Kim et al., 2020; Sheridan et al., 2020). A variety of morphogens and growth factors are added to the organoid culture media to recapitulate the *in vivo* chemical conditions experienced by the organ of interest during different

stages of development (Corsini & Knoblich, 2022). For the placenta, this means aggregating CT cells and providing them with the necessary conditions for ST cell differentiation (Sheridan et al., 2020). Differentiation of EVT along with ST cells within these organoids is also feasible with minor modifications to the culture media (Dietrich et al., 2023).

2. Research objectives

My project focuses on elucidating the role of GDF15 on human placental development using organoids grown from human trophoblast stem cells. By culturing wildtype (WT), homozygous GDF15 gene knockout (KO), and heterozygous GDF15 gene knockout ($GDF15^{+/-}$) CT cells and trophoblast organoids, I hope to answer the following questions:

1. Does GDF15 impact the proliferation and differentiation of placental stem cells?
2. Is the ratio of CT to ST cells in human trophoblast organoids impacted by GDF15?

3. Methods and Materials

3.1 Trophoblast stem cell culture

Previous collaboration with the Genome Engineering Facility at the Max Planck Institute of Molecular Cell Biology and Genetics (Dresden, Germany) has generated multiple GDF15 knockout CT29 cell clones using CRISPR/Cas9-mediated gene disruption technology. The CT29 cells, obtained originally from RIKEN cell bank, are human trophoblast stem cells and are capable of differentiating into various placental cell types (Okae et al., 2018). The success of the gene editing process in these GDF15

knockout clones has been confirmed by PCR or Sanger Sequencing. Mock edited (WT), heterozygous GDF15 knockout ($GDF15^{+/-}$), and homozygous GDF15 knockout (KO) cell clones of CT29 cells were transported to the Xing lab prior to my involvement with the lab, and these are the cells I used for my project.

2D cell cultures of WT, $GDF15^{+/-}$ and KO CT29 cell clones were grown in multiwell cell culture plates (Nunc Cell Culture, Thermo Fisher Scientific) in an incubator set to 37 °C and 5% CO_2. A layer of diluted Geltrex™ (Thermo Fisher Scientific; diluted to 0.08mg/ml in Advanced DMEM/F12) was added to each well before cells were seeded. Geltrex™ is a commercial basement membrane matrix that mimics the naturally occurring extracellular matrix and helps with cell attachment and growth (Alshareeda et al., 2025). Table 1 shows the amount of Geltrex™, and media used in various multiwell cell culture plates used throughout this experiment.

Table 1. Multiwell cell culture plate size, the amount of Geltrex™ used, and the amount of media used in each well. Geltrex™/well was determined based on preliminary experiments and media/well was determined based on manufacturer recommendations.

Well plate size	**Geltrex™/well**	**Media/well**
6-well plate	1.5 ml	2 ml
12-well plate	1 ml	1.5 ml
24-well plate	750 µl	750 µl
48-well plate	500 µl	500 µl

The cells were fed DMEM/F-12 nutrient mixture cell culture media supplemented with the items listed in Table 2 as per the recipe published in Okae et al. (2018). The cells were monitored daily using the EVOS M3000 microscope, and the media was changed on Mondays, Wednesdays, and Fridays. When the cell clusters had expanded to cover 70-90% of the well's surface, known as reaching 70-90% confluency, the cells were detached from the well using a commercially available enzymatic solution called TrypLE™ Express (Gibco, Thermo Fisher Scientific). This process suspends the previously adherent cells in solution and, following centrifugation, the cell pellet can be resuspended in fresh media and divided into new wells at a 1:2 ratio. This process of transferring cells from confluent wells into new, empty wells is called passaging.

Table 2. Reagents used for 2D CT29 cell culture. Published by Okae et al. in 2018.

Reagent	Concentration	Company	Catalogue Number
DMEM/F-12 nutrient mixture *	1x	Life Technologies Inc	11320033
2-mercaptoethanol *	0.1mM	Thermo Fisher Scientific	AC125472500
Penicillin-Streptomycin *	0.5X	Gibco	15070-063
Bovine serum albumin (BSA) *	0.3%	Millipore Sigma	A8412-100ML
Fetal bovine serum (FBS) *	0.2%	Gibco	12483020
Valproic acid *	0.8 mM	STEMCELL Technologies	100-1053
Insulin-Transferrin-Selenium-Ethanolamine supplement	1x	Life Technologies Inc	51500056
L-ascorbic acid	1.5 µg/ml	Thermo Fisher Scientific	FLA61-100
Human epidermal growth factor (EGF)	50 ng/ml	Thermo Fisher Scientific	AF-100-15-100UG
CHIR99021	2 µM	Millipore Sigma	361571-5MG
A83-01	0.5 µM	Millipore Sigma	SML0788-5MG
SB431542	1 µM	EMD Milipore Corp	61 646 45MG
Y-27632 ROCK inhibitor **	10 µM for thawing or passaging, 5µM for media change	ABMOLE	M1817-5MG

* Combined and filtered through a 0.22 µm PVDF syringe filter before the remaining ingredients are added

** Added fresh every time

3.2 Trophoblast organoid culture

After establishing the 2D cultures, trophoblast organoids were generated using WT, GDF15$^{+/-}$ and KO CT29 cell clones, following a previously published protocol (Sheridan et al., 2020), with minor modifications. Briefly, CT29 cells were dissociated from culture plates and resuspended in 25 μL Geltrex^{TM} droplets at a seeding density of 2,500 cells per droplet. One droplet was added to each well of an 8-well chamber slide, as depicted in Figure 1. These droplets were surrounded by trophoblast organoid media (TOM) composed of Advanced DMEM/F-12 and various supplements, listed in Table 3. Cells in Geltrex^{TM} droplets grew and differentiated to form trophoblast organoids over time. The organoids were monitored daily, and the media was changed on Mondays, Wednesdays, and Fridays. Three batches of organoids were grown for this project. The first contained GDF15$^{+/-}$ organoids and was maintained in culture for 15 days before being fixed in 4% paraformaldehyde (PFA). Batch two contained WT and KO organoids and was maintained for 36 days before fixation. Batch 3 contained WT and GDF15$^{+/-}$ organoids and was maintained for 28 days before fixation. By culturing organoids with different genotypes in the same batch, variation in culture conditions is reduced, and the organoids can be compared more reliably.

Table 3. Reagents used for trophoblast organoid culture. Published by Sheridan et al. in 2020.

Reagent	Concentration	Company	Catalogue Number
Advanced DMEM/F12	1x	Gibco	12634-010
N2 supplement	1x	Gibco	17502048
B27 supplement minus vitamin A	1x	Gibco	17504044
L-glutamine	2 mM	Millipore Sigma	G7513-100ML
N-Acetyl-L-Cysteine	1.25 mM	Millipore Sigma	A9165-5G
Primocin	100 µg/ml	Cedarlane	ANT-PM-2
Human fibroblast growth factor 2 (FGF2)	100 ng/ml	Peprotech	100-18B
R-Spondin	80 ng/ml	Peprotech	120-38-100
EGF	50 ng/ml	Peprotech	AF-100-15-100UG
Human hepatocyte growth factor (HGF)	50 ng/ml	Peprotech	100-39H-100UG
Prostaglandin E2	2.5 µM	Thermo Fisher Scientific	233560100
CHIR99021	1.5 µM	Millipore Sigma	361571-5MG
Y-27632 ROCK inhibitor	2 µM	ABMOLE	M1817-5MG
A83-01	500 nM	Millipore Sigma	SML0788-5MG

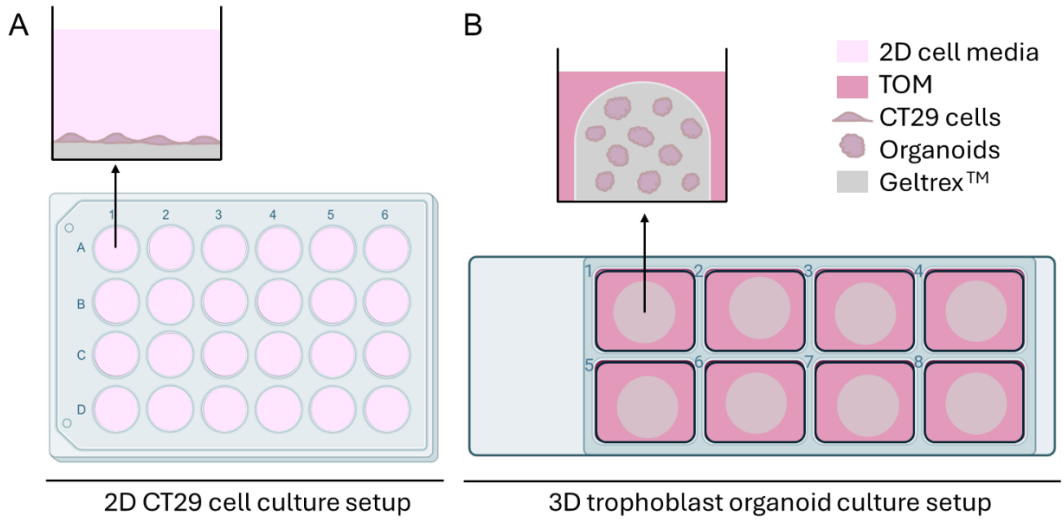


Figure 1. Model setup of the 2D CT29 cell culture and 3D trophoblast organoid culture. A) 2D CT29 cell culture set up showing the 2D cell media, CT29 cells, and Geltrex™. Cells are grown in multiwell cell culture plates ranging from 6 wells/plate to 24 wells/plate. B) 3D trophoblast organoid culture setup showing the TOM, trophoblast organoids, and Geltrex™. Organoids are grown in 8-well chamber slides.

3.3 Cell proliferation assay

The proliferative abilities of WT and KO CT29 cells in the presence and absence of human recombinant GDF15 protein were tested using the Click-iT Plus EdU Alexa Fluor 555 Imaging Kit (Thermo Fisher Scientific). Table 4 describes the GDF15 concentration and administration duration for all CT29 cell clones used for this experiment. Each KO clone (clones 7 and 11) was grown in two wells: one received supplemental GDF15 with every media change, and the other did not. Only one well of the WT clone (clone 6) was grown. The supplemented wells of both KO clones were exposed to 100 ng/ml of GDF15 for 8 days. Clone 7 well 1 received an additional 5 days of exposure to 200 ng/ml. This double dose was tested because it was not visually

apparent that the initial dosage was having any effect on increasing proliferation or slowing colony death.

5-ethynyl 2′-deoxyuridine (EdU) is a nucleoside analog of thymidine that cells can incorporate into their DNA when performing DNA synthesis. The cells in culture were incubated with 10 μM EdU for 24 hours, followed by fixation in 3.7% PFA and storage at -20 °C in methanol until further analysis. Following the kit protocol, EdU was detected in the cells' DNA using a copper (I) catalyzed click chemistry reaction, where the alkynes in EdU covalently bind to azides in Alexa Fluor 555 fluorescent dyes. All cell nuclei that were in S-phase during the EdU incubation are thereby stained and detected using a fluorescent microscope. All cells were also stained with Hoechst 33342, a DNA dye that marks all cell nuclei in culture, regardless of whether or not they were performing DNA synthesis.

Table 4. Cell clones used for the cell proliferation assay.

Clone and well number	Genotype	Supplemental GDF15 concentration	Duration
6, well 1	WT	None	N/A
7, well 1	KO	100 ng/ml; 200 ng/ml	8 days; 5 days
7, well 2	KO	None	N/A
11, well 1	KO	100 ng/ml	8 days
11, well 2	KO	None	N/A

Cell counting was automated using FIJI. The Hoechst 33342 and EdU images were analyzed separately after minimal editing. After converting an image to grayscale, a

threshold was applied to distinguish cells from the background and generate a binary image where cells were black, and the background was white. The staining was extremely clear, and this threshold was very simple to implement. Overlapping cells were separated using the watershed program, and cells were counted using the 'Analyze Particles' function. A map of the outline of each cell was generated following the counting. This map allowed the automated counting to be verified manually through comparison to the original image, and small changes could be made to get a more accurate count.

3.4 Immunofluorescence

The same staining procedure was used for cells and for organoids. Following fixation in 4% PFA, the samples were washed in 1x phosphate-buffered saline (PBS) twice for five minutes, permeabilized in 0.3% TritonX100 in 1x PBS at room temperature for 5 minutes, washed in Tx blocking buffer at room temperature for 1 hour, and stained with primary antibodies for E-cadherin (CDH1, Cell Signaling Technology 3195S), staining the CT cells, and for the beta 3 subunit of human chorionic gonadotropin (CGB3, Abcam ab9582), staining ST cells, at a dilution of 1:500 in Tx blocking buffer overnight in a humid chamber at 4°C. The following morning, the samples were washed in Tx blocking buffer 3 times for 10 minutes each time. Next, they were incubated with secondary antibodies (Mouse 488, Invitrogen; Rabbit 555, Invitrogen) at a dilution of 1:500 and DAPI at a dilution of 1:1000 for 1 hour at room temperature, protected from light. Following three 10-minute washes in PBS, the samples were either mounted with Mowiol or left in PBS if mounting was impossible. Clone 6 cells, clone 7 cells, and batch 2 organoids were mounted in Mowiol, while clone 11 cells and batch 3 organoids were left in PBS because they were grown in vessels incompatible with the cover slips

available to me. For all organoid batches, one well of organoids from each genotype were used as negative controls, where primary antibodies were omitted. Bright field images of organoids were taken using an EVOS M3000 microscope; immunostained organoids were imaged using a Zeiss LSM700 confocal microscope (batch 2) and an EVOS M7000 microscope (batch 3).

Quantification of these images was performed manually in FIJI using the cell counter plugin. Images were edited using comparable settings, and counting was performed blinded. Area measurements were also obtained using FIJI.

3.5 Statistical analysis

Data processing, statistical analysis, and figure illustration were performed using Excel (Microsoft) and Prism (GraphPad Software). The Kolmogorov–Smirnov and Shapiro–Wilk tests were used to assess normality in the data, and equality of variance was confirmed using the F-test. Normally distributed data were analyzed using two-tailed unpaired Student's t-tests or one-way analysis of variance (ANOVA) tests, followed by post hoc Tukey's multiple comparison tests. If the data were not normally distributed or failed to have equal variances, the Mann-Whitney U test or the Kruskal-Wallis test was used to compare groups. Fisher's exact test was used to analyze contingency data.

4. Results

4.1 Establishment of CT29 cell 2D culture

Following the cell culture methods I proposed, WT, GDF15$^{+/-}$ and KO CT29 cell clones were grown in 2D cultures. Cell health was assessed visually after every media change and passage. Figure 2 shows typical growth for a healthy cell clone (Clone 6, WT)

over one week. After seeding, many small clusters and lone CT29 cells spread throughout the well. After a few days, a central cluster (Fig. 2A) begins to form, along with a few smaller peripheral clusters. As time passes, the central cluster expands while most of the peripheral clusters and lone cells die off or are absorbed by the central mass (Fig. 2B-D). Most, if not all, cells should display the phenotype highlighted in the green box in Figure 3. Cells that resemble those in the red box in Figure 3 frequently die off and are replaced by healthier cells. A well full of unhealthy-looking cells suggests serious problems with the culture conditions. These cells do not proliferate well and may be differentiated ST cells.

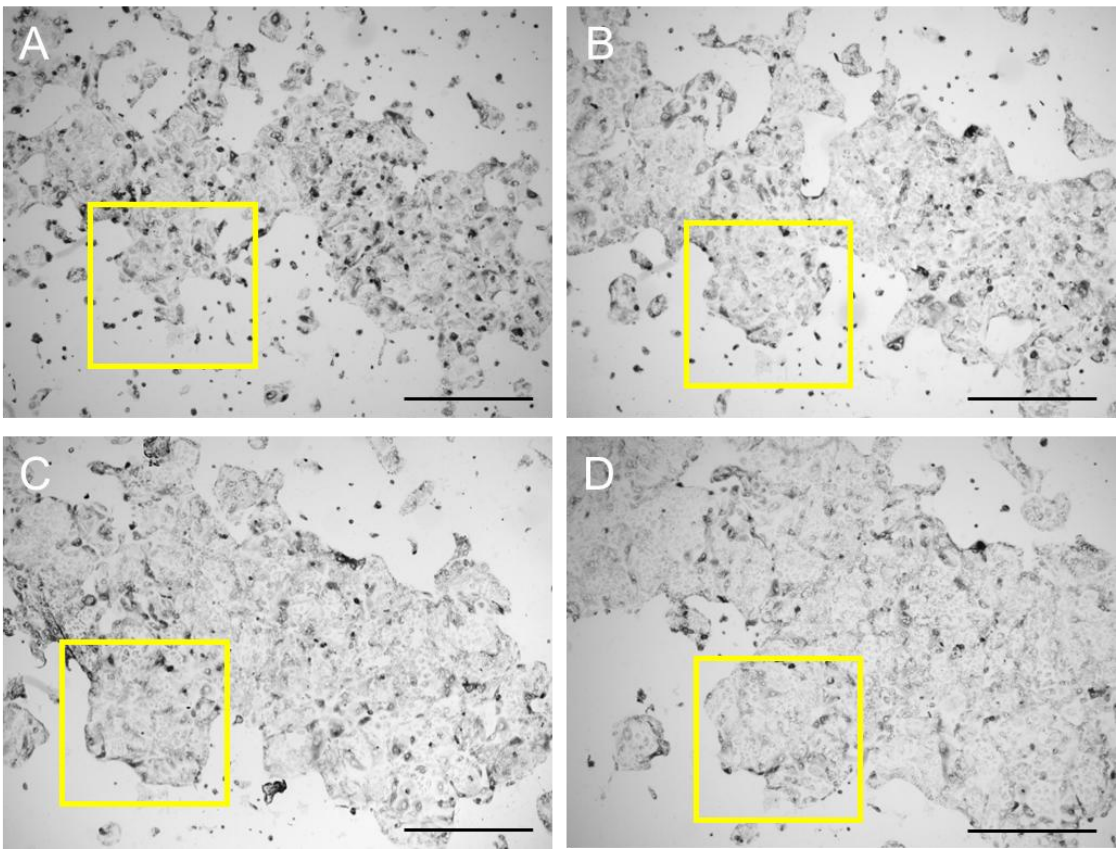


Figure 2. Light microscopy images of typical CT29 cell growth taken at 4X magnification. One large cluster and many smaller peripheral cell clusters of Clone 6 CT29 cells (WT) imaged on day 2 (A), day 4 (B), day 6 (C) and day 8 (D) after initial seeding. Growth and expansion of cells in the main cluster, and the disappearance of lone cells, are visible in the boxed area on different days. Scale bar = 1500 µm.

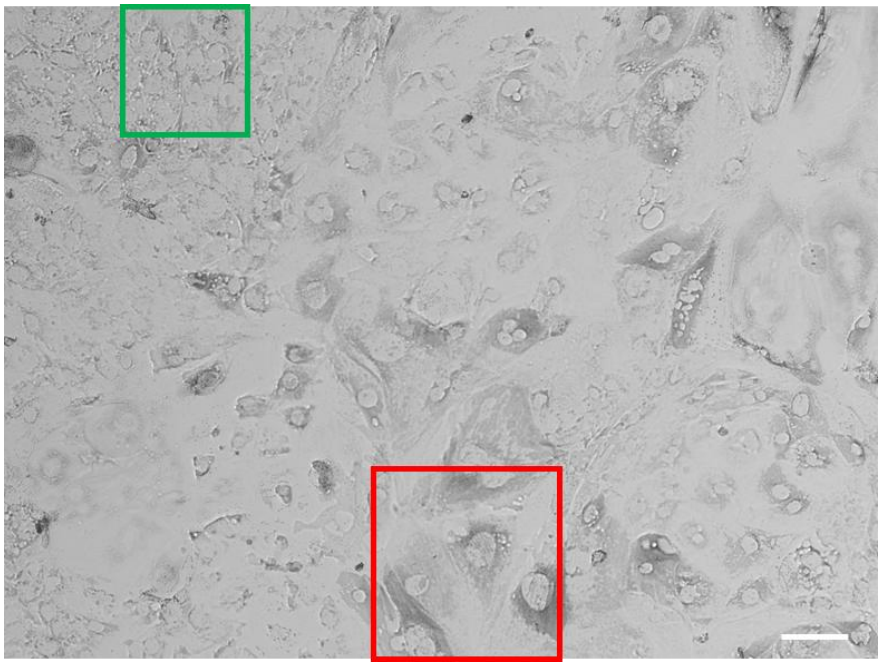


Figure 3. Image of a WT CT29 cell cluster taken at 10X magnification. The green box shows cells displaying a healthy phenotype (small, light-coloured, round, tightly clustered), while the red box shows cells displaying a less healthy phenotype (large, dark-coloured, elongated). Cells in the red box would be expected to die off unless they were clustered together with healthier cells, as in this case. Scale bar = 100 µm.

4.2 GDF15 deficiency impairs CT29 cell growth

To quantify the growth of different CT29 cell clones, I attempted to construct growth curves using the relative colony size in well plates as the evaluation parameter. Relative size was determined based on one well in a 6-well plate being equivalent to two wells in a 12-well plate or four wells in a 24-well plate. A value of '1' on this scale represents one 70% confluent well in a 24-well plate. Therefore, a value of '2' could represent either two 70% confluent wells in a 24-well plate or one 70% confluent well in a 12-well plate. An ideal growth curve for these cell clones is expected to increase

exponentially, as each well reaches confluency and its cells are reseeded into larger or more new wells. However, since cells are removed from the system for experiments (organoid production, RNA extraction, etc.) and for cryopreservation (to maintain frozen aliquots in case the colony fails), the actual growth curves deviate markedly from the ideal. All clones were given the same media at the same frequency and grown in the same incubator, yet some were more difficult to maintain than others, suggesting a genotype effect on proliferation or hardiness.

Growth curves with decreasing sections that cannot be accounted for by experiments or freezing are indicated with stars in Figure 4. More unexpected decreases are observed in Figure 4C than in Figure 4B. The drop in Figure 4B, indicated by the star, was likely due to an error at the start of the culture: the seeding density was much lower than optimal. Clone 6 was transferred to a smaller well in a (successful) attempt to rescue it before it could die off. Clone 14 was unable to survive a similar error and died off soon after being passaged. This illustrates one example of how the three KO clones failed to thrive and exhibited significantly impaired growth compared with WT clones cultured under the same conditions. Both WT clones 6 and 4 started growing soon after passaging into appropriately sized well plates and were used in experiments. The GDF15$^{+/-}$ clone 17 also grew well and was quickly used for experiments before being cryopreserved for future use. Both KO clones 11 and 14 showed much slower growth at the beginning of the culture. While KO clone 7 initially showed growth comparable to the WT clones, it soon began to decline as well. The KO clones also showed a reduced growth rate, indicated by the longer interval between data points (passages). All three KO clones failed to survive in culture and died off or were terminated when it became obvious that they were not growing properly. This inspired further research using an EdU proliferation assay to

investigate proliferation in WT and KO cells, as the growth curves suggested that GDF15 KO may have reduced the proliferative abilities of CT29 cells.

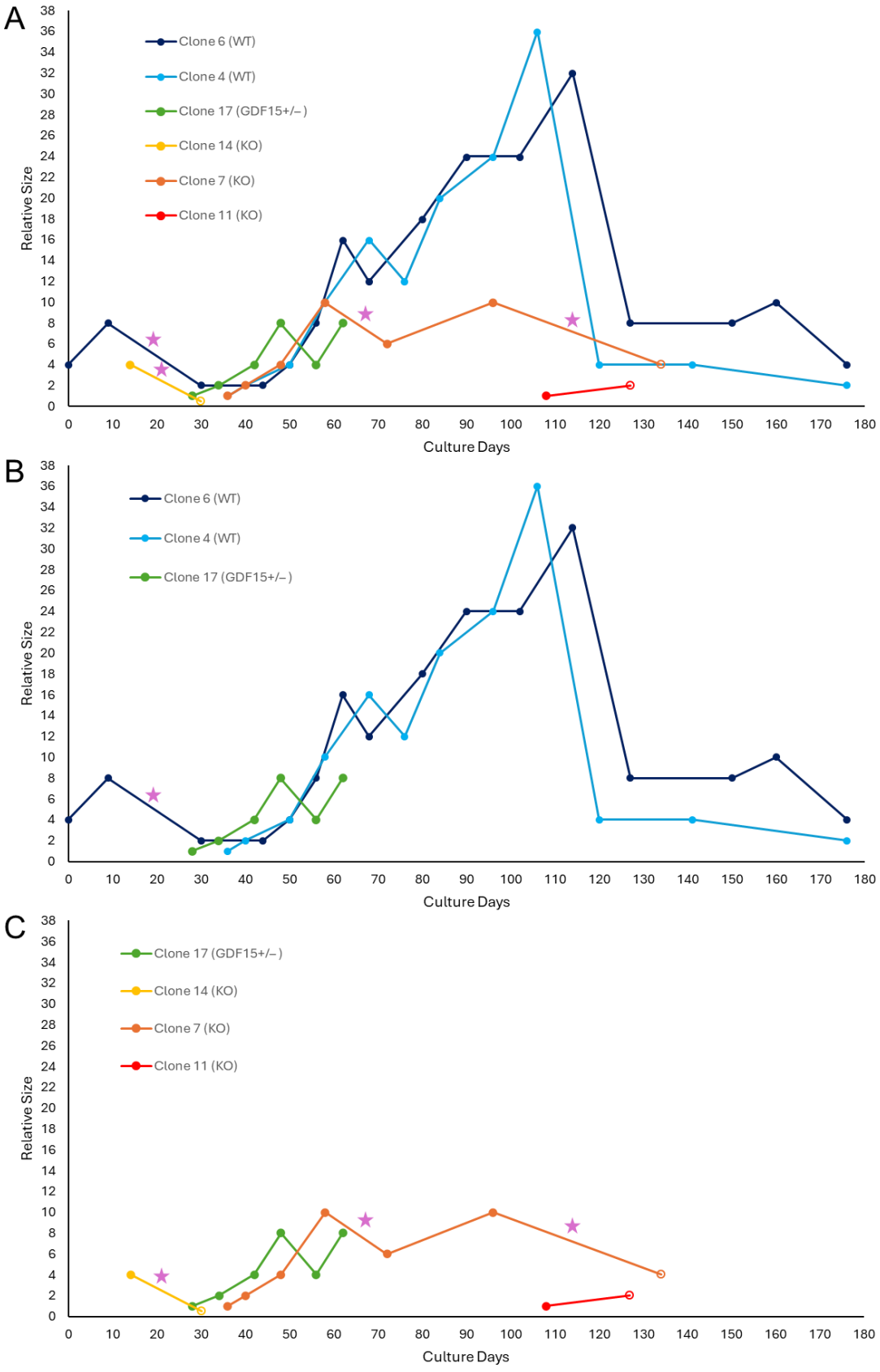

A
Clone 6 (WT)
Clone 4 (WT)
Clone 17 (GDF15+/–)
Clone 14 (KO)
Clone 7 (KO)
Clone 11 (KO)
Relative Size
Culture Days
B
Clone 6 (WT)
Clone 4 (WT)
Clone 17 (GDF15+/–)
Relative Size
Culture Days
C
Clone 17 (GDF15+/–)
Clone 14 (KO)
Clone 7 (KO)
Clone 11 (KO)
Relative Size
Culture Days

Figure 4. Growth curves of different CT29 cell clones. A) Two WT clones (Clone 6 in navy and Clone 4 in light blue), three KO clones (Clone 14 in yellow, Clone 7 in Orange, and Clone 11 in red), and one GDF15$^{+/-}$ clone (Clone 17 in green) are shown in the graph. The relative size of the cell colony is used as an evaluation parameter; a 70%-90% confluent well in a 24-well plate is defined as 1, which is shown on the Y-axis. Culture days are shown on the X-axis. Solid circle symbols indicate times when cells were passaged and collected for experiments or cryopreservation, as needed. Hollow circle symbols indicate the last passage of a clone before death or terminal experiments. Each curve begins at passage 0, after the clone was thawed from cryopreservation. Stars indicate colony size decreases that were not due to cell collection for organoid culture, experimentation, or cryopreservation. B) shows only the WT and GDF15$^{+/-}$ clones, while C) shows only the KO and GDF15$^{+/-}$ clones for ease of comparison.

4.3 GDF15 deficiency decreases CT29 cell proliferation

Prompted by the growth curve data, I performed a cell proliferation assay using the Click-iT Plus EdU Alexa Fluor 555 Imaging Kit. As shown in Figure 5, Clone 6 (WT) had a significantly higher ratio of EdU+ cells to total cells in culture, compared to both KO clones, regardless of whether they received supplemental GDF15. This is consistent with the growth curve data, suggesting that GDF15 deficiency reduced the proliferative capacity of CT29 cells. Clone 11 KO GDF15+ has more EdU+ cells compared to Clone 11 KO, but Clone 7 did not significantly benefit from the addition of GDF15. The WT clone 6 had significantly more EdU+ cells than both KO treatment groups, and GDF15

supplementation led to a significant increase in EdU+ cells compared to the unsupplemented KO group, when the data from both clones was combined (Figure 5C).

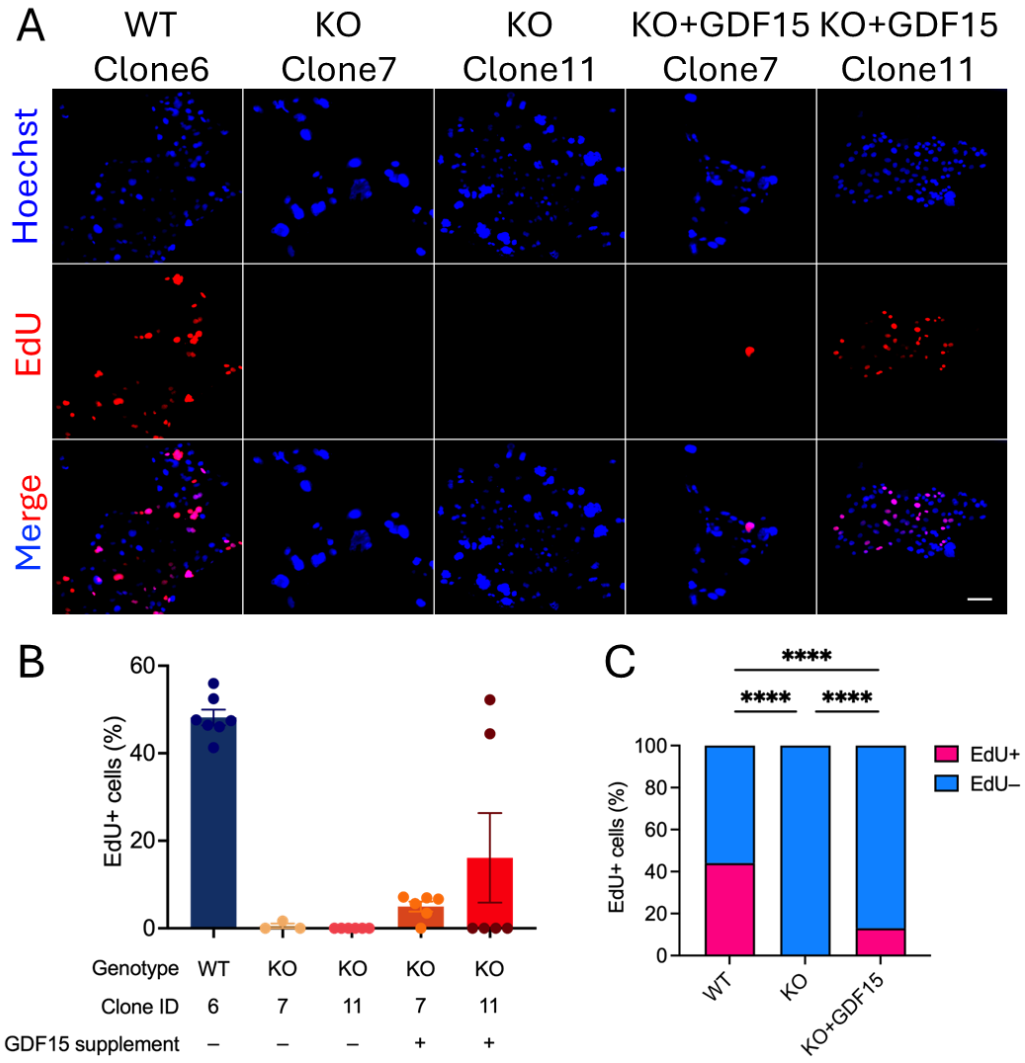


Figure 5. GDF15 regulates CT29 cell proliferation. A) EdU (red; marks proliferating cells) and Hoechst 33342 (blue; marks all cell nuclei) staining across three CT29 cell clones from two genotypes (WT and KO). KO clones were divided into two treatments: GDF15-supplemented (KO+GDF15) and not (KO). Scale bar = 50µm. B) Bar representing the average percentage of EdU+ cells in WT clone 6 (navy), KO clone 7 (beige), KO clone 11 (pink), KO clone 7 GDF15+ (orange), and KO clone 11 GDF15+

(red). The points show the percentage from each sample of the five groups. The percentage of EdU+ cells was calculated by dividing the number of EdU+ cells by all cells (identified by Hoechst 33342 staining) in each image. Sample sizes: Clone 6 n =7 (2790 cells total), Clone 7 n = 3 (190 cells total), Clone 11 n = 6 (329 cells total), Clone 7 GDF15+ n = 6 (400 cells total), and Clone 11 GDF15+ n = 6 (243 cells total). Error bars = standard error of the mean. C) The average percentage of EdU+ and EdU- cells across three GDF15 treatments: untreated WT cells producing their own GDF15 (WT; n = 7; 2790 cells total), untreated KO cells KO; n = 9; 519 cells total), and GDF15-supplemented KO cells (KO+GDF15; n = 12; 643 cells total). All three groups are significantly different, as indicated by asterisks.

4.4 Establishment of 3D trophoblast organoid culture

Following the methods outlined above, I grew three batches of trophoblast organoids. The first batch contained 8 GDF15$^{+/-}$ droplets on a single chamber slide, one droplet per chamber. This batch was grown to familiarize myself with the protocol. The second batch contained 4 WT and 4 KO droplets on the same chamber slide, one droplet per chamber. The third batch has 4 WT and 4 GDF15$^{+/-}$ droplets in the same chamber slide, one droplet per chamber. While batches 1 and 2 were grown on chamber slides with removable walls (leading to a flat microscope slide at the time of imaging), batch 3 was grown in a chamber slide with non-detachable walls. This chamber slide came pre-coated with collagen IV, which helps with cell adhesion to the well floor. I had had difficulties keeping the Geltrex^{TM} attached to the well floor, particularly at the corners of the wells in previous batches, so this new chamber slide was selected to potentially solve this issue. Unfortunately, since the chamber walls could not be removed, I could not image these

organoids using the confocal microscope without risking damage to the objectives. I instead had to use an epifluorescence microscope (EVOS M7000 by Thermo Fisher Scientific), which does not provide the same resolution. Further, I could only use 4x and 10x objectives, since the higher magnification objectives are short-range and require the slide to be flipped upside down. This was impossible, as the chamber slides were filled with PBS for long-term storage, and the chamber walls prevented me from mounting a coverslip properly. As a result, the organoids appear very small in each image, and it is difficult or impossible to distinguish which individual cells are positive or negative for CDH1 or CGB3. Therefore, batch 3 organoids were excluded from quantitative analysis.

When comparing organoids from batch 2 (Figures 6 and 7), KO organoids exhibited a delayed growth rate compared to WT organoids. Despite the WT organoids reaching the target diameter of 200-300 μm, I kept the batch in culture longer to see whether KO organoids would continue to grow. Unfortunately, this was never achieved, and the batch was removed from culture when the organoids began to deteriorate, as shown in Figure 7. Over 36 days in culture, the KO organoids remained small, likely due to the decreased proliferative capacity of KO CT29 cells, as explained previously. The WT organoids grew and then began shrinking as they deteriorated from being in culture too long. There were also more organoids in the WT wells compared to the KO wells, even though the same number of CT29 cells were used to initiate organoid culture.

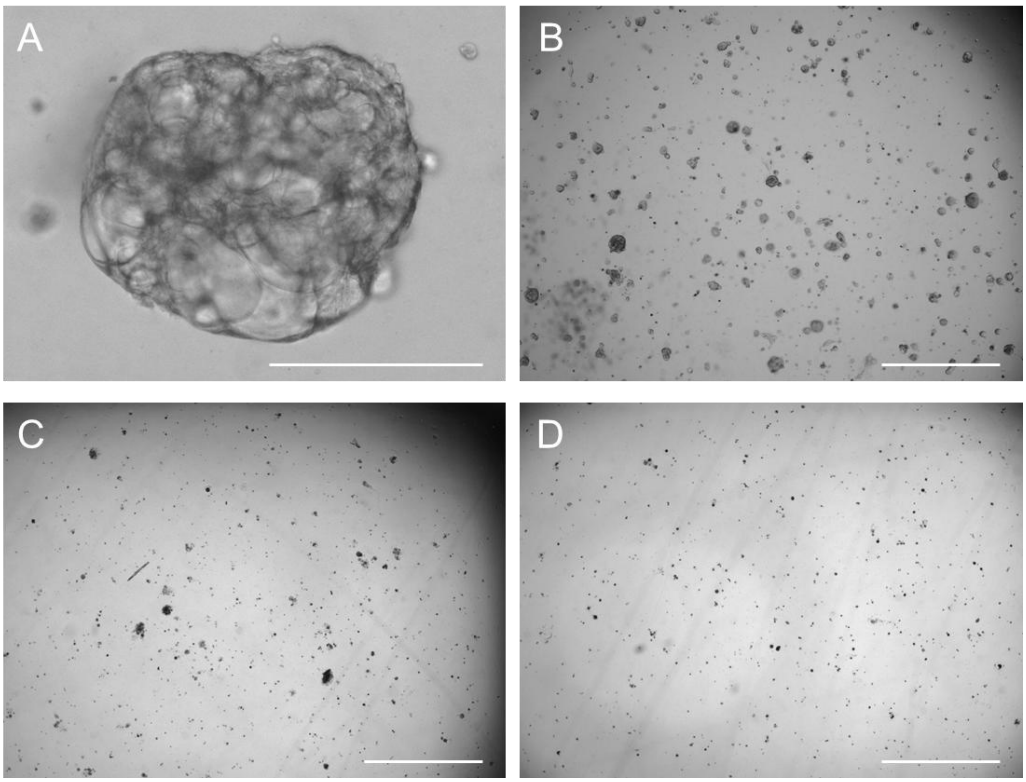


Figure 6. Brightfield images of trophoblast organoids and droplets in culture. A) 20X magnification image of one representative organoid within the GDF15$^{+/-}$ droplet from batch 1. B) 4X magnification image of one batch 1 GDF15$^{+/-}$ droplet 12 days after seeding. C) 4X magnification image of one WT droplet 36 days after seeding. D) 4X magnification image of one KO droplet 36 days after seeding. The organoids in C and D have begun deteriorating and are less representative of a healthy droplet compared to A and B. Images were taken using the EVOS M3000 microscope, Scale bar A = 200 µm, B-D = 1500 µm.

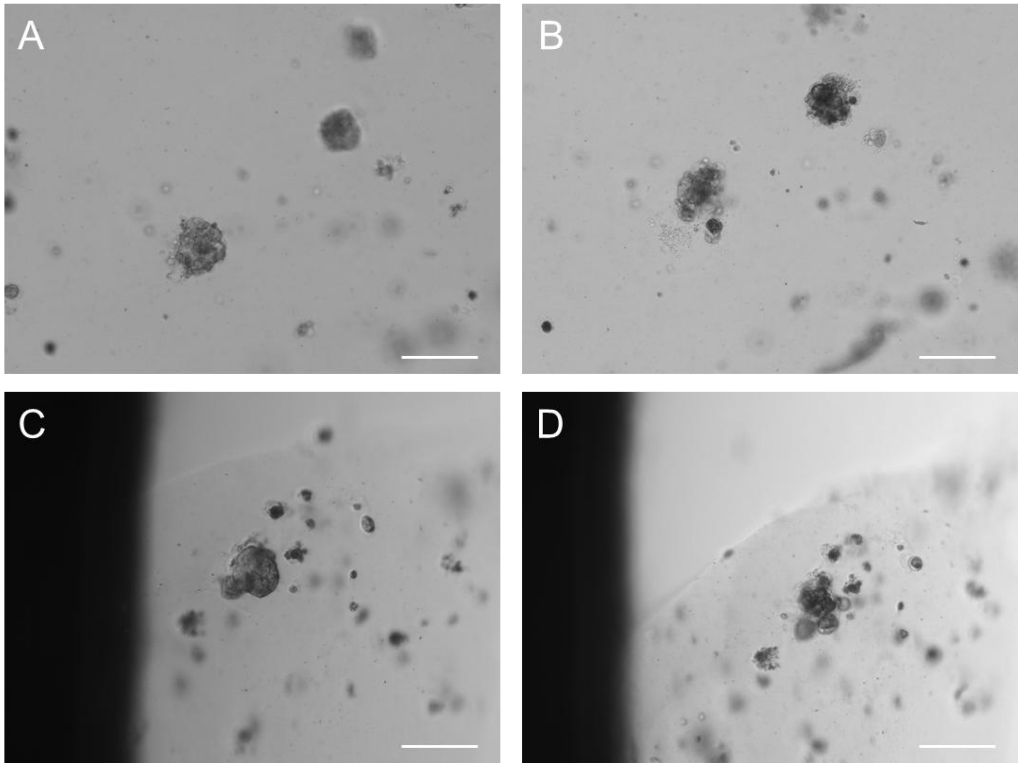


Figure 7. Brightfield images of trophoblast organoids in culture. 10X magnification images of WT (A and B) and KO (C and D) organoids 19 days (A and C) and 36 days (B and D) after seeding. This KO organoid was one of the largest in the batch, while the WT organoids are average-sized. By day 36, all organoids showed signs of deterioration: dark and loosely clustered. Images were taken using the EVOS M3000 microscope. Scale bar = 200 μm.

4.5 Area of WT, KO, and GDF15$^{+/-}$ organoids

Batches 2 and 3 remained in culture for comparable durations and contained three genotypes in total. Despite the difficulties in imaging batch 3, I hoped to compare these groups in some way. The area of organoids grown in these batches could be obtained using FIJI and potentially compared across the three genotypes. To ensure data comparability, I first compared WT organoids from both batches. Unfortunately, their

mean areas differed by orders of magnitude, which made me doubt that further comparisons would be valuable. I suspect that factors other than genotype, such as the collagen IV coating, clone-to-clone variation, cell passage number, or batch variation in various media components, affected organoid size. Furthermore, the WT organoids in batch 2 shrank over time, while the KO organoids failed to grow. This represents a temporal change which could not be captured by comparing their area at the time of fixation. Batch-to-batch variation in organoid research is often significant, and I decided against continuing these comparisons. Table 5 shows the average area (and standard deviation) for organoids in all three genotypes in batches 2 and 3.

Statistical analysis comparing WT and KO organoids in batch 2 showed unequal variance and non-significant results in a Mann-Whitney U test comparison. By increasing the sample sizes in all categories, variance would potentially shrink, and the statistical power would improve. Growing more organoids for comparisons is definitely a goal for future study, expanding these findings.

Table 5. Average area of WT, KO, and GDF15$^{+/-}$ organoids grown in two batches.

Batch	Genotype	Average Area (μm^2)	Standard deviation	Sample Sizes
2	WT	14,136.94	8,539.02	6
	KO	7,529.38	1,802.84	4
3	WT	665.37	241.10	4
	GDF15$^{+/-}$	1,029.50	417.11	4

4.6 Ratio of CT and ST cells in WT and KO organoids

Figure 8 shows representative images of WT and KO trophoblast organoids generated from clone 4 (WT) and clone 7 (KO) CT29 cells. Initially, across all batch 2 organoids, the WT organoids appeared to have a higher proportion of CDH1+ cells, suggesting greater CT cell abundance and a larger stem cell pool to support further organoid growth. In contrast, the KO organoids appeared to show greater CGB3 staining, suggesting a higher proportion of differentiated ST cells. The WT organoids were also larger than the KO organoids, despite having already begun to shrink and deteriorate by the time these images were taken.

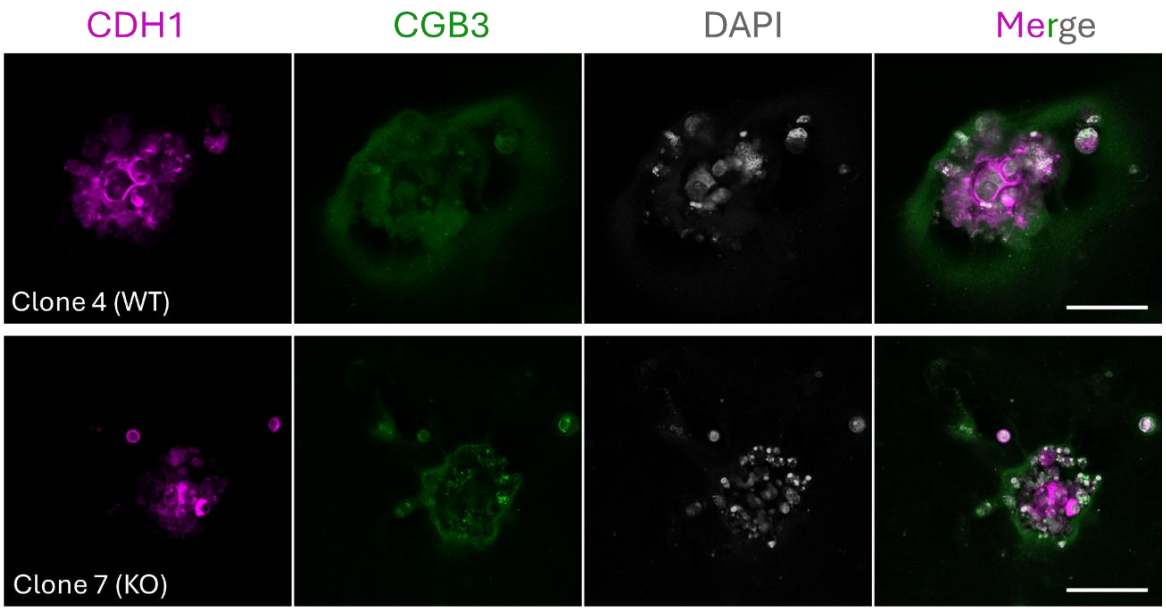


Figure 8. Representative images of WT (Clone 4) and KO (Clone 7) organoids stained with CDH1 (pink), CGB3 (green), and DAPI (grey). Images taken using a confocal microscope. Scale bar = 100µm.

However, quantitative analysis does not fully support these qualitative assessments. Figure 9 shows the quantification of batch 2 WT and KO organoids based on CDH1 and CGB3 expression. Cells expressing only CDH1 are CT cells, while cells expressing only CGB3 are ST cells. Cells expressing both are likely in the process of differentiating and therefore still express some CDH1 even as they acquire CGB3 expression. Cells that express neither marker may be other cell types, or they may not be expressing these markers in the focal plane assessed, despite expressing them elsewhere. The proportion of CDH1+ cells (Figure 9.A) was not significantly different between the WT and KO groups, although the p-value may improve if more samples are assessed. This is also the case for the CGB3+/DAPI and CDH1+CGB3–/DAPI groups (Figure 9. B and C). The proportion of CDH1–CGB3+ cells (Figure 9. D) is significantly higher in the KO group. This means that a higher proportion of cells in KO organoids are ST cells, compared to the proportion of ST cells in WT organoids. This suggests that the KO organoids favour differentiation more than the WT organoids. If the CDH1+CGB3– cells were significantly different between the two groups, this would mean that the ratio of CT to ST cells is higher in WT compared to KO organoids. Without this significance, further research is necessary to confirm this statement; however, given the p-value and the small sample sizes, I suspect this claim is true. This aligns with my findings concerning how GDF15 regulates CT cell proliferation in the 2D culture experiments. The KO organoids lack GDF15, thereby reducing the proliferative capacity of CT cells, promoting CT-to-ST differentiation, and increasing the proportion of ST cells.

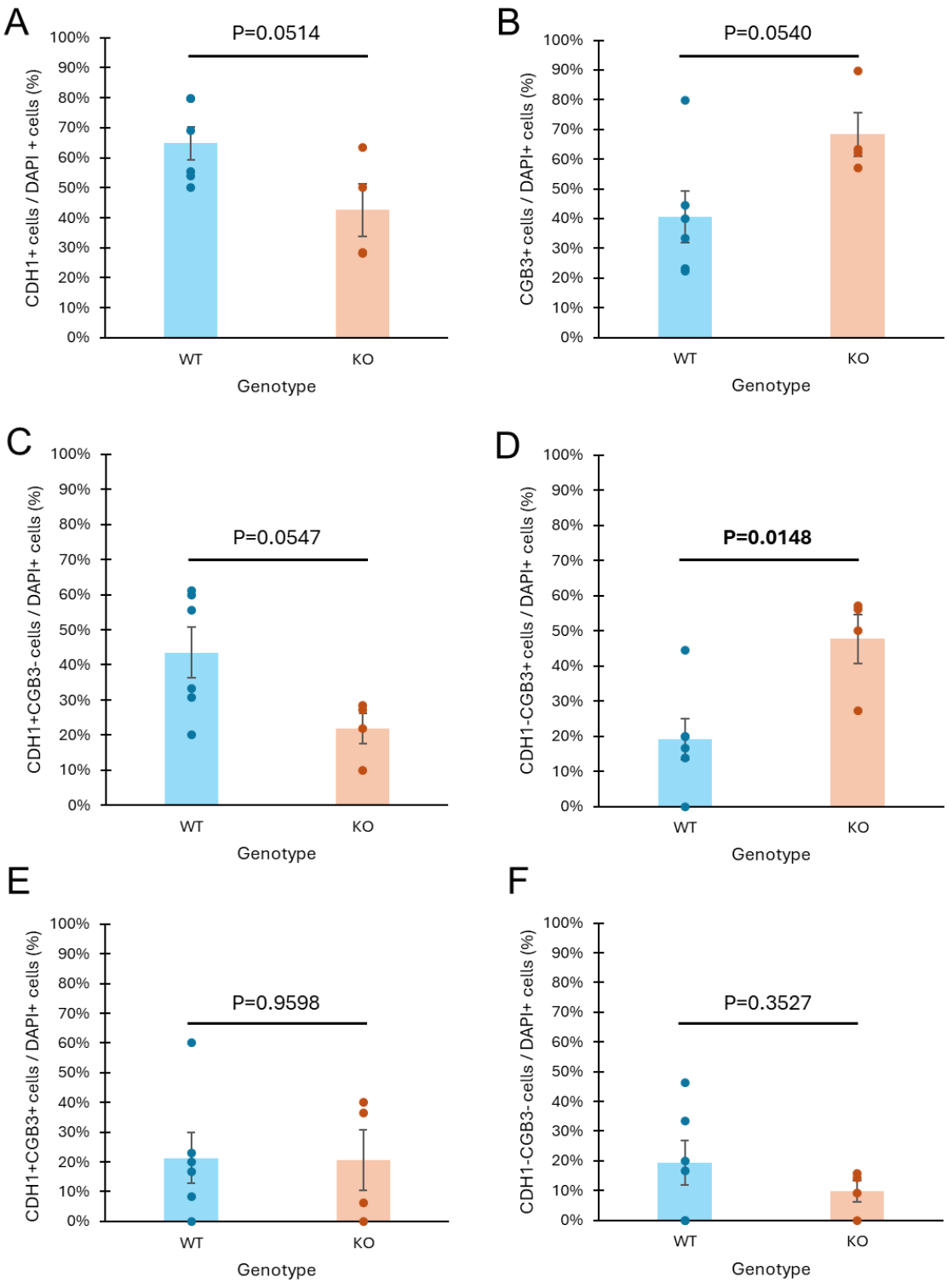

A
P=0.0514
CDH1+ cells / DAPI + cells (%)
100%
90%
80%
70%
60%
50%
40%
30%
20%
10%
0%
WT
KO
Genotype
B
P=0.0540
CGB3+ cells / DAPI+ cells (%)
C
P=0.0547
CDH1+CGB3- cells / DAPI+ cells (%)
D
P=0.0148
CDH1-CGB3+ cells / DAPI+ cells (%)
E
P=0.9598
CDH1+CGB3+ cells / DAPI+ cells (%)
F
P=0.3527
CDH1-CGB3- cells / DAPI+ cells (%)

Figure 9. GDF15 deficiency increases the proportion of ST cells in trophoblast organoids. A) Cells positive for CDH1 divided by cells positive for DAPI (total cell number). B) Cells positive for CGB3 over DAPI. C) Cells positive for CDH1 but negative for CGB3 over DAPI. These are CT cells in the trophoblast organoids. D) Cells negative for CDH1, but positive for CGB3 over DAPI. These are ST cells in the trophoblast organoids. E) Cells positive for both CDH1 and CGB3 over DAPI. These double-positive cells are in the process of differentiating from CT cells to ST cells. F) Cells negative for both CDH1 and CGB3 over DAPI. These double-negative cells are neither CT nor ST, nor are they in the process of differentiating. Sample sizes: WT n = 6 organoids (74 cells), KO n = 4 organoids (60 cells). Error bars = standard error of the mean.

Quantification was hindered by a high CGB3 background in both genotypes. This complicated the assessment of both CGB3+ and CGB3– cells because it was difficult to distinguish the positive signal from the background. In some cases, the Geltrex™ appears to have lifted off the chamber slide floor and folded near the well walls. This is likely a consequence of prolonged culture, leading to increased manipulation of the wells and degradation of components within Geltrex™. These folds had a very strong CGB3 signal, sometimes as strong as the positive signal coming from the ST cells in the surrounding organoids. I am not entirely sure why Geltrex™ showed such high CGB3 staining in some cases but not in others. The ST cells secrete HCG, which could theoretically have been trapped under folded or lifted Geltrex™, leading to the positive staining. However, HCG would likely be rapidly degraded in the organoid media, and numerous wash steps during the immunofluorescence staining protocol should have removed any residual secreted hormones. I could not find any literature on CGB3 staining in Geltrex™, and I

did not observe it in all of my samples, suggesting this isn't a problem with the compound itself.

Batch 3 organoids were excluded from quantitative analysis due to the technical problems explained above, but this batch also showed non-specific staining and high background for CGB3. Some of this background could have also been coming from interactions with the collagen IV coating, but again, I didn't find examples of this phenomenon in the literature. Organoids in this batch were also kept in culture longer than is ideal, and the Geltrex^{TM} may have become saturated with HCG during this time, which would also explain why batch 1 did not have such a high CGB3 background signal.

5. Discussion

GDF15 appears to be critical for maintaining the proliferative abilities of CT29 cells, both in 2D culture and in 3D trophoblast organoids. In its absence, CT29 cells fail to thrive, leading to colony death as cells stop proliferating. A rescue effect was observed when KO colonies recovered their proliferative abilities following supplementation of recombinant GDF15 into culture media. Further, without GDF15, organoids were slow to develop and favoured differentiation into ST cells rather than proliferation to produce more CT cells. This prohibits long-term growth as the pool of CT stem cells is exhausted. Furthermore, WT organoids grew and then shrank while KO organoids failed to grow at all. Even so, WT organoids were larger compared to KO organoids grown in the same batch. Overall, this points to the importance of GDF15 in the proliferation of trophoblast stem cells and the development of the human placenta.

GDF15 is known to promote migration and invasion in both ST and EVT cells, but little is known about its effects on CT cells, particularly the general molecular

mechanisms underpinning CT cell behaviour, such as proliferation (Schäffers et al., 2025; Yang et al., 2025; Zeng et al., 2023). Given the limited research on the effects of GDF15 on CT cells, results from studies using other growth factors and cell types can be compared with my findings to assess the validity of my conclusions. Some growth factors, such as EGF, enhance CT cell proliferation, whereas others, such as transforming growth factor β1, promote differentiation (Li & Zhuang, 1997). A member of the same superfamily as GDF15, bone morphogenetic protein 4, is used to transform human embryonic stem cells into CT cells, which can later differentiate into ST and EVT cells, suggesting its role in specifying the trophoblast lineage but not necessarily in the maintenance of stemness in CT cells (Li et al., 2013). The effects of all growth factors or members of the TGF-β superfamily on CT cells are therefore not identical, again highlighting the need for studies specifically focused on GDF15. Research on other cell types, including epithelial cells, shows that GDF15 promotes proliferation, which aligns with my findings (Li et al., 2018; Van Huyen et al., 2008). Specifically, the addition of recombinant human GDF15 to the media of cervical cancer cells grown *in vitro* promoted their proliferation and improved their viability through paracrine and autocrine signalling (Li et al., 2018). Paracrine signalling involves short-distance cell communication, which would be facilitated in large cell clusters. If the effects of GDF15 on proliferation are modulated through paracrine signalling, this may explain why the greatest improvement was seen in the largest clusters of clone 11 KO+GDF15 cells. Paracrine signaling between small, distant cell clusters would be difficult, potentially limiting the success of the GDF15 rescue effect; the larger clone 11 KO+GDF15 clusters would have improved paracrine signaling capacities, promoting rescue. This pattern also suggests that GDF15

rescue may be more successful when added to cells seeded at high density, where they are more likely to cluster, as I have seen in this project.

There are numerous ways to assess the proliferative capacity of CT cells, but one of the most effective is to directly measure DNA synthesis (Flomerfelt & Gress, 2016). Nucleoside-analog incorporation assays allow cells to incorporate chemically or radioactively labelled nucleosides (such as tritiated thymidine, 5-bromo-2′-deoxyuridine, or EdU) into their DNA during the S phase of the cell cycle (Romar et al., 2016). The use of EdU has grown in popularity since it does not require DNA denaturation, has an extremely low signal-to-noise ratio, and generates highly reproducible results (Flomerfelt & Gress, 2016). This method has been performed using genetically modified trophoblast cells *in vitro*, confirming its applicability for the present study (Chu et al., 2022). The detection of EdU in cultured cells has also been used in chondrocytes supplemented with GDF15 at the same concentrations I used (Wang et al., 2022). While my results do not indicate improved proliferative ability at higher GDF15 doses (I found no dose dependent effects between the 200 ng/ml supplementation in clone 7 KO+GDF15 compared to 100 ng/ml in clone 11 KO+GDF15), Wang et al. (2022) found significant differences among the WT, 100 ng/ml GDF15, and 200 ng/ml GDF15 groups. Clone 7, which was incubated with 200 ng/ml GDF15 during its final five days in culture, had been steadily dying for longer than Clone 11, and it may have been too far gone for a dose-dependent rescue effect to be seen. Clone 7 responded poorly to the rescue effect of 200 ng/ml GDF15 compared to clone 11, potentially due to its extremely low proliferative capacity and survival rate, which may have exceeded the point of rescue. Nevertheless, the rescue effect had a positive effect on both clones, even if minor in the case of clone 7. Further experiments using CT29 GDF15 KO cells supplemented with different concentrations of

GDF15 should account for potential effects of cluster size and compare clones that have been deteriorating for the same duration. Another limitation of my study was that both KO clones only received supplemental GDF15 after their lack of proliferation was confirmed over many days in culture. If GDF15 had been provided earlier in their demise, the rescue may have been more successful. Nevertheless, my findings point to the efficacy of GDF15 rescue in GDF15 KO CT29 cells, further suggesting a role for GDF15 in CT cell proliferation.

Next, I sought to determine whether the absence of GDF15 promotes CT cells differentiation into ST cells. I used the novel trophoblast organoid model system to understand the dynamics between CT and ST cell abundance in 3D cultures. While 2D cell culture-based experiments provide valuable findings, translational differences occur when moving to more complex *in vivo* systems. Organoids serve as an excellent intermediate model system between *in vitro* and *in vivo*, allowing for the verification that mechanisms discovered in classic cell culture are maintained in 3D environments containing multiple cell types and more complex cell-to-cell interactions (Hu et al., 2026). This is especially relevant when differences between humans and non-human animal models may be significant, as is the case in placental research, given the unique evolution of human placentation, particularly when compared to mice and other common laboratory models (Carter, 2021). Furthermore, by validating discoveries in more complex systems, your findings gain further credibility. For example, Li et al. (2018) found that implanting GDF15-overexpressing cervical cancer cells into mice led to greater tumour growth compared to controls, corroborating their earlier results pertaining to the proliferation-promoting effects of GDF15 *in vitro* and establishing the applicability of their findings from 2D cell culture experiments to *in vivo* systems.

In the present study, I found that in the absence of GDF15, trophoblast organoids generate a larger proportion of differentiated ST cells compared to controls. A recent study found that GDF15 levels secreted from organoids into their media are lower when the organoid protocol is aimed at promoting differentiation into EVT compared to cases where organoids are developing solely into CT and ST cells (Wessel et al., 2025). This suggests that low GDF15 allows for differentiation, but higher levels are correlated with organoids maintaining a larger pool of CT cells, which would be generated through proliferation. The effects of GDF15 on signalling cascades relating to the differentiation of stem cells are also under study (Tanno et al., 2011; Kim et al., 2025; Zhu et al., 2021). The overexpression of GDF15 inhibits the differentiation of human adipocytes through HOP2-mediated suppression of CCAAT/enhancer binding protein α, which is a transcription factor implicated in the differentiation of numerous cell types (Kim et al., 2025). It has also been shown that GDF15 upregulates the expression of leukemia inhibitor factor (LIF), which promotes the maintenance of a stem-cell state and induces self-renewing proliferative divisions rather than differentiative divisions (Zhu et al., 2021). One of the most widely cited stem-cell-associated transcription factors, SOX2, can also be induced by GDF15, further supporting the role of GDF15 in promoting self-renewing divisions (Tanno et al., 2011). My finding that the absence of GDF15 pushes CT cells in trophoblast organoids towards more differentiative divisions, generating ST cells, is very much in line with known effects of GDF15 on division modes. Collectively, my findings indicate that GDF15 not only promotes the proliferation of CT29 cells but also inhibits their differentiation, helping to preserve a pool of stem cells that allows for larger and potentially healthier organoids. Having identified this effect, I hope that future research continues investigating which signalling pathways are activated in trophoblast

stem cells specifically, and which molecular mechanisms are behind the rescue effect of GDF15 supplementation on GDF15 KO cells, as observed in my 2D culture experiments.

One key limitation of this study was the length of time batch 2 and 3 organoids spent in culture. Signs of deterioration were evident in both batches, which potentially led to smaller organoids, especially in the WT condition. Small organoids are more likely to die off, contributing fewer organoids to assess and unhealthy phenotypes in survivors (Sheridan et al., 2020). However, considering this from an alternative perspective, the effect of the absence of GDF15 was so strong that organoids produced from the KO cells would barely grow. The KO organoids also had a higher proportion of ST cells, suggesting that their stem cell pool was reduced in favour of differentiative divisions. This would also contribute to their smaller overall size since a reduction in proliferative divisions would limit growth substantially.

Furthermore, despite the many benefits of using organoids for research, this remains a relatively new model system, and further work is needed to optimize all protocols used. One of the major hurdles to large-scale organoid experiments is the lack of uniformity and, consequently, reproducibility across batches (Zhang et al., 2023). Size and external morphology are the most common variables affected by both within- and between-batch variation, as was clearly seen in my experiments (Velasco et al., 2019). This is especially problematic when characterizing the effects of an understudied factor, such as GDF15, because it becomes harder to distinguish normal variation from genotype-dependent variation when there is so little literature on the topic. Furthermore, necessary components for organoid formation, such as Geltrex^{TM}, FBS, and BSA, exhibit inherent batch-to-batch variation in protein content and concentration, which may not be well tolerated by all cell types (Foster et al., 2025; Gstraunthaler et al., 2013). Some studies

have found that along with biochemical components (proteins, growth factors, etc.), mechanical properties (stiffness, density, etc.) associated with 3D matrices like Geltrex™ can alter gene expression in cells, even changing differentiation pathways in stem cells (Foster et al., 2025; Zonderland & Moroni, 2021). While improving reproducibility is an active area of study for some organoid models, trophoblast organoids have yet to receive such attention (Velasco et al., 2019; Zhang et al., 2023). Fortunately, the huge potential of organoids as model systems has inspired many researchers to investigate ways to improve comparability between batches. By standardizing experimental conditions (growing organoids of various genotypes in the same culture well, using the same media aliquots, keeping time spent in culture as similar as possible, generating mock-edited cells for controls, etc.) and increasing sample sizes, statistical analysis can identify significant differences caused by treatments rather than natural variation. Until the factors contributing to batch-to-batch variation in trophoblast organoids are fully characterized, all conclusions drawn from multi-batch experiments should be interpreted with caution. However, all models come with caveats, and if reported clearly, this should not dissuade the use of these valuable systems. This is especially significant for studies on humans since any conclusions drawn from other animal models would come with their own set of unavoidable limitations pertaining to species differences. Filling the research gap of identifying ways to ensure comparability between multi-batch organoid experiments is beyond the scope of any one project and requires the continued work of the many researchers in this field.

The placenta is a critically understudied organ. Investigation into its constituent cell types and how cell-extrinsic factors impact its development and the progression of pregnancy could fill research gaps in the fields of basic human biology and obstetric

health. Returning to my research objectives, GDF15 impacts the proliferation of placental stem cells, as shown by my 2D culture experiments. Furthermore, the ratio of CT to ST cells in human trophoblast organoids is impacted by GDF15, since in its absence, trophoblast organoids produced proportionally more differentiated ST cells. Despite limited sample sizes and the inability to compare $GDF15^{+/-}$ organoids, this study concludes that GDF15 is an essential component for healthy placental development, promoting CT cell proliferation in 2D and 3D organoid cultures. Following genetic knockout, CT29 cell clusters and organoids developed abnormally, suggesting negative consequences in the *in vivo* placenta. Luckily, a rescue effect was discovered, opening further opportunities for research into this organ and growth factor. This would be an instrumental discovery for further work to pursue, given the association between low GDF15 and pregnancy complications like preeclampsia (Chen et al., 2016). The therapeutic potential of GDF15 analogues for treating obesity and various metabolic diseases is currently under study, and perhaps further research should explore their potential for treating preeclampsia as well (Wang et al., 2021).

6. References

Alshareeda, A. T., Albarakati, N., Alshawakir, Y., Alghuwainem, A., Al-Sowayan, B. S., Khan, A. L., Almubarak, A., Al-Maiman, S., Al Sayed, A., Mohd Zin, N. K., & Alhamid, A. S. (2025). Improving the robustness and efficiency of cell sheet protocol for breast cancer induction in animal model: A Geltrex plus Gelatin approach. *PLOS One*, *20*(6), e0326456. https://doi.org/10.1371/journal.pone.0326456

Carter, A. M. (2007). Animal models of human placentation – A review. *Placenta, 28*, S41–S47. https://doi.org/10.1016/j.placenta.2006.11.002

Carter, A. M. (2021). Unique aspects of human placentation. *International Journal of Molecular Sciences*, *22*(15), 8099. https://doi.org/10.3390/ijms22158099

Chen, Q., Wang, Y., Zhao, M., Hyett, J., da Silva Costa, F., & Nie, G. (2016). Serum levels of GDF15 are reduced in preeclampsia and the reduction is more profound in late-onset than early-onset cases. *Cytokine*, *83*, 226–230. https://doi.org/10.1016/j.cyto.2016.05.002

Chu, Z., Wang, Y., Zhang, S., & Cao, P. (2022). Circ_0004904 suppresses trophoblast cell proliferation, invasion and migration in preeclampsia via upregulating the expression of DNA damage inducible alpha by interacting with miR-19a-3p. *Cell Cycle*, *22*(4), 464–475. https://doi.org/10.1080/15384101.2022.2124616

Corsini, N. S., & Knoblich, J. A. (2022). Human organoids: New strategies and methods for analyzing human development and disease. *Cell*, *185*(15), 2756–2769. https://doi.org/10.1016/j.cell.2022.06.051

Fejzo, M., Rocha, N., Cimino, I., Lockhart, S. M., Petry, C. J., Kay, R. G., Burling, K., Barker, P., George, A. L., Yasara, N., Premawardhena, A., Gong, S., Cook, E., Rimmington, D., Rainbow, K., Withers, D. J., Cortessis, V., Mullin, P. M.,

MacGibbon, K. W., … O'Rahilly, S. (2024). GDF15 linked to maternal risk of nausea and vomiting during pregnancy. *Nature*, *625*(7996), 760–767. https://doi.org/10.1038/s41586-023-06921-9

Flomerfelt, F. A., & Gress, R. E. (2016). Analysis of cell proliferation and homeostasis using EdU labeling. *Methods in Molecular Biology (Clifton, N.J.)*, *1323*, 211–220. https://doi.org/10.1007/978-1-4939-2809-5_18

Gstraunthaler, G., Lindl, T., & van der Valk, J. (2013). A plea to reduce or replace fetal bovine serum in cell culture media. *Cytotechnology*, *65*(5), 791–793. https://doi.org/10.1007/s10616-013-9633-8

Gumusoglu, S. B. (2024). The role of the placenta-brain axis in psychoneuroimmune programming. *Brain, Behavior, & Immunity - Health*, *36*, 100735. https://doi.org/10.1016/j.bbih.2024.100735

Herrick, E. J., & Bordoni, B. (2023). Embryology, Placenta. In *StatPearls*. StatPearls Publishing. http://www.ncbi.nlm.nih.gov/books/NBK551634/

Hu, X., Xie, Y., Wang, J., Zhang, X., & Wu, R. (2026). Development and transformation of veterinary experimental in vitro models: From 2D culture to 3D organoids. *Animals : An Open Access Journal from MDPI*, *16*(3), 469. https://doi.org/10.3390/ani16030469

Iglesias, P., Silvestre, R. A., & Díez, J. J. (2023). Growth differentiation factor 15 (GDF-15) in endocrinology. *Endocrine*, *81*(3), 419–431. https://doi.org/10.1007/s12020-023-03377-9

Jin, C., Peng, Y., Luo, X., Zhu, Q., Lin, L., Yang, J., & Wang, P. (2025). Dynamic change of estrogen and progesterone metabolites in human urine during pregnancy. *Scientific Reports*, *15*, 8409. https://doi.org/10.1038/s41598-025-92866-0

Kay, V. R., Rätsep, M. T., Cahill, L. S., Hickman, A. F., Zavan, B., Newport, M. E., Ellegood, J., Laliberte, C. L., Reynolds, J. N., Carmeliet, P., Tayade, C., Sled, J. G., & Croy, B. A. (2018). Effects of placental growth factor deficiency on behavior, neuroanatomy, and cerebrovasculature of mice. *Physiological Genomics*, *50*(10), 862–875. https://doi.org/10.1152/physiolgenomics.00076.2018

Kim, J., Koo, B.-K., & Knoblich, J. A. (2020). Human organoids: Model systems for human biology and medicine. *Nature Reviews Molecular Cell Biology*, *21*(10), 571–584. https://doi.org/10.1038/s41580-020-0259-3.

Kim, H. J., Kang, S.-U., Kim, H. J., Lee, Y. S., & Kim, C.-H. (2025). GDF15 inhibits early-stage adipocyte differentiation by enhancing HOP2 expression and suppressing C/EBPα expression. *Molecular and Cellular Endocrinology*, *598*, 112461. https://doi.org/10.1016/j.mce.2025.112461

Li, R. H., & Zhuang, L. Z. (1997). The effects of growth factors on human normal placental cytotrophoblast cell proliferation. *Human Reproduction*, *12*(4), 830–834. https://doi.org/10.1093/humrep/12.4.830

Li, S., Ma, Y.-M., Zheng, P.-S., & Zhang, P. (2018). GDF15 promotes the proliferation of cervical cancer cells by phosphorylating AKT1 and Erk1/2 through the receptor ErbB2. *Journal of Experimental & Clinical Cancer Research*, *37*(1), 80. https://doi.org/10.1186/s13046-018-0744-0

Li, X., Li, Z.-H., Wang, Y.-X., & Liu, T.-H. (2023). A comprehensive review of human trophoblast fusion models: Recent developments and challenges. *Cell Death Discovery*, *9*(1), 372. https://doi.org/10.1038/s41420-023-01670-0

Li, Y., Moretto-Zita, M., Soncin, F., Wakeland, A., Wolfe, L., Leon-Garcia, S., Pandian, R., Pizzo, D., Cui, L., Nazor, K., Loring, J. F., Crum, C. P., Laurent, L. C., & Parast,

M. M. (2013). BMP4-directed trophoblast differentiation of human embryonic stem cells is mediated through a ΔNp63+ cytotrophoblast stem cell state. *Development*, *140*(19), 3965–3976. https://doi.org/10.1242/dev.092155

Mischler, A., Karakis, V., Mahinthakumar, J., Carberry, C. K., San Miguel, A., Rager, J. E., Fry, R. C., & Rao, B. M. (2021). Two distinct trophectoderm lineage stem cells from human pluripotent stem cells. *The Journal of Biological Chemistry*, *296*, 100386. https://doi.org/10.1016/j.jbc.2021.100386

Novakovic, B., Gordon, L., Robinson, W. P., Desoye, G., & Saffery, R. (2013). Glucose as a fetal nutrient: Dynamic regulation of several glucose transporter genes by DNA methylation in the human placenta across gestation. *The Journal of Nutritional Biochemistry, 24*(1), 282–288. https://doi.org/10.1016/j.jnutbio.2012.06.006

Nursalim, Y. N. S., Groom, K. M., Blenkiron, C., & Chamley, L. W. (2021). A simple method to isolate term trophoblasts and maintain them in extended culture. *Placenta, 108*, 1–10. https://doi.org/10.1016/j.placenta.2021.03.009

Okae, H., Toh, H., Sato, T., Hiura, H., Takahashi, S., Shirane, K., Kabayama, Y., Suyama, M., Sasaki, H., & Arima, T. (2018). Derivation of human trophoblast stem cells. *Cell Stem Cell*, *22*(1), 50-63.e6. https://doi.org/10.1016/j.stem.2017.11.004

Romar, G. A., Kupper, T. S., & Divito, S. J. (2016). Research techniques made simple: techniques to assess cell proliferation. *Journal of Investigative Dermatology*, *136*(1), e1–e7. https://doi.org/10.1016/j.jid.2015.11.020

Rosenfeld, C. S. (2021). The placenta-brain-axis. *Journal of Neuroscience Research*, *99*(1), 271–283. https://doi.org/10.1002/jnr.24603

Sato, K. (2013). Placenta-derived hypo-serotonin situations in the developing forebrain cause autism. *Medical Hypotheses, 80*(4), 368–372. https://doi.org/10.1016/j.mehy.2013.01.002

Schäffers, O., Verburgt, S., Harhangi, M., Broekhuizen, M., Hengel, E. van, Meeren, L. van der, Schoenmakers, S., Dekkers, D., Doff, W., Demmers, J., Reiss, I., Gribnau, J., & Rijn, B. van. (2025). *Characterization of cytotrophoblast cell population dynamics throughout pregnancy* (p. 2025.01.22.634235). bioRxiv. https://doi.org/10.1101/2025.01.22.634235

Sheridan, M. A., Fernando, R. C., Gardner, L., Hollinshead, M. S., Burton, G. J., Moffett, A., & Turco, M. Y. (2020). Establishment and differentiation of long-term trophoblast organoid cultures from the human placenta. *Nature Protocols*, *15*(10), 3441–3463. https://doi.org/10.1038/s41596-020-0381-x

Shin, H., Wong, E. S., Gohr, A., Ray, S., Morris, S., Mohamad, R., Derihaci, R. P., Wimberger, P., Strelau, J., Huttner, W. B., & Xing, L. (2026). *Placenta-derived growth differentiation factor 15 promotes neural progenitor proliferation in the developing mammalian neocortex*. Cell Reports (CELL-REPORTS-D-26-00043, in revision)

Tanno, T., Merchant, A., Agarwal, J. R., Wang, Q., & Matsui, W. (2011). The TGF- β family member growth differentiation factor 15 (GDF15) regulates the self-renewal of multiple myeloma cancer stem cells. *Blood*, *118*(21), 2954. https://doi.org/10.1182/blood.V118.21.2954.2954

Turco, M. Y., & Moffett, A. (2019). Development of the human placenta. *Development*, *146*(22), dev163428. https://doi.org/10.1242/dev.163428

Vacher, C.-M., Lacaille, H., O'Reilly, J. J., Salzbank, J., Bakalar, D., Sebaoui, S., Liere, P., Clarkson-Paredes, C., Sasaki, T., Sathyanesan, A., Kratimenos, P., Ellegood, J.,

Lerch, J. P., Imamura, Y., Popratiloff, A., Hashimoto-Torii, K., Gallo, V., Schumacher, M., & Penn, A. A. (2021). Placental endocrine function shapes cerebellar development and social behavior. *Nature Neuroscience*, *24*(10), 1392–1401. https://doi.org/10.1038/s41593-021-00896-4

Van Huyen, J. P. D., Cheval, L., Bloch-Faure, M., Belair, M. F., Heudes, D., Bruneval, P., & Doucet, A. (2008). GDF15 triggers homeostatic proliferation of acid-secreting collecting duct cells. *Journal of the American Society of Nephrology : JASN*, *19*(10), 1965–1974. https://doi.org/10.1681/ASN.2007070781

Velasco, S., Kedaigle, A. J., Simmons, S. K., Nash, A., Rocha, M., Quadrato, G., Paulsen, B., Nguyen, L., Adiconis, X., Regev, A., Levin, J. Z., & Arlotta, P. (2019). Individual brain organoids reproducibly form cell diversity of the human cerebral cortex. *Nature*, *570*(7762), 523–527. https://doi.org/10.1038/s41586-019-1289-x

Wang, D., Day, E. A., Townsend, L. K., Djordjevic, D., Jørgensen, S. B., & Steinberg, G. R. (2021). GDF15: Emerging biology and therapeutic applications for obesity and cardiometabolic disease. *Nature Reviews Endocrinology*, *17*(10), 592–607. https://doi.org/10.1038/s41574-021-00529-7

Wang, D., Wei, X., Geng, X., Li, P., & Li, L. (2022). GDF15 enhances proliferation of aged chondrocytes by phosphorylating SMAD2. *Journal of Orthopaedic Science*, *27*(1), 249–256. https://doi.org/10.1016/j.jos.2020.12.004

Wessel, B. M., Castro, J. N., Harrison, H. F., Scottoline, B. P., Wilcox, M. C., Baldwin, M. K., & Roberts, V. H. J. (2025). Development of a trophoblast organoid resource in a translational primate model. *Organoids*, *4*(4), 24. https://doi.org/10.3390/organoids4040024

Yang, S.-H., Yang, L., Shi, Y., Xu, H.-R., Gan, J., Shi, J.-X., Zhang, Y., Shen, S.-L., Wang, J., & Zhang, X. (2025). GDF15 promotes trophoblast invasion and pregnancy success via the BMPR1A/BMPR2/p-SMAD1 pathway: Implications for recurrent miscarriage. *Life Sciences*, *371*, 123586. https://doi.org/10.1016/j.lfs.2025.123586

Zeng, Y.-T., Liu, W.-F., Zheng, P.-S., & Li, S. (2023). GDF15 deficiency hinders human trophoblast invasion to mediate pregnancy loss through downregulating Smad1/5 phosphorylation. *iScience*, *26*(10), 107902. https://doi.org/10.1016/j.isci.2023.107902

Zhang, X.-S., Xie, G., Ma, H., Ding, S., Wu, Y.-X., Fei, Y., Cheng, Q., Huang, Y., & Wang, Y. (2023). Highly reproducible and cost-effective one-pot organoid differentiation using a novel platform based on PF-127 triggered spheroid assembly. *Biofabrication*, *15*(4), 045014. https://doi.org/10.1088/1758-5090/acee21

Zhu, S., Yang, N., Guan, Y., Wang, X., Zang, G., Lv, X., Deng, S., Wang, W., Li, T., & Chen, J. (2021). GDF15 promotes glioma stem cell-like phenotype via regulation of ERK1/2–c-Fos–LIF signaling. *Cell Death Discovery*, *7*, 3. https://doi.org/10.1038/s41420-020-00395-8

Zonderland, J., & Moroni, L. (2021). Steering cell behavior through mechanobiology in 3D: A regenerative medicine perspective. *Biomaterials*, *268*, 120572. https://doi.org/10.1016/j.biomaterials.2020.120572